Research Article GU J Sci 38(3): x-x (2025) DOI: 10.35378/gujs.1653428

Gazi University

Journal of Science

http://dergipark.gov.tr/gujs

Structural and Dielectric Properties of Pristine Bentonite-PVC Nanocomposites

Ahmet Uğur KAYA*

Kocaeli University, Department of Physics, 41001, Kocaeli, Türkiye

Highlights

- XRD and FTIR analyses confirmed the partial intercalation of PVC into bentonite layers.
- PVC loading altered permittivity, dielectric loss, and relaxation, mainly at low frequencies.
- Interfacial polarization and mobility variations suggest PVC-bentonite use in insulation.

Article Info

Received: 07 Mar 2025
Accepted: 24 Apr 2025

Keywords

Bentonite-PVC nanocomposites,
Dielectric properties,
Intercalation and surface interactions,
Electrode polarization,
Structural analyses

Abstract

In this study, the structural and dielectric properties of pristine bentonite-PVC (Polyvinyl chloride) nanocomposites were systematically investigated. X-ray diffraction (XRD) and Fourier transform infrared spectroscopy (FTIR) analyses confirmed the partial intercalation of PVC molecules between the bentonite layers and their interaction with surface hydroxyl groups. The dielectric properties of the nanocomposites were examined via impedance spectroscopy over a broad frequency range of 1 Hz–10 MHz. The results revealed that PVC loading significantly influenced dielectric permittivity, dielectric loss, and loss tangent (tan δ). At low frequencies (<1 kHz), the permittivity and dielectric loss values of 25 mg, 35 mg, and 100 mg PVC-loaded nanocomposites were notably higher compared to pristine bentonite, indicating enhanced interfacial polarization. The relaxation frequency of pristine bentonite was determined to be 39 kHz, which shifted to lower frequencies upon polymer loading due to intercalation and surface interactions. Notably, in the 35 mg PVC-loaded nanocomposite, the relaxation frequency decreased to 12 kHz, suggesting stronger polymer-clay interactions. In addition, AC conductivity (σ_{ac}) analyses were performed and successfully fitted with the Jonscher power law, confirming the dominant role of interfacial polarization and dipolar confinement on charge transport behavior. These findings demonstrate that the dielectric behavior of PVC-bentonite nanocomposites is governed by both intercalation and surface interactions, which modulate charge carrier mobility and polarization mechanisms. The integration of structural (XRD, FTIR) and dielectric (impedance spectroscopy) analyses provides a comprehensive understanding of the impact of polymer loading on the dielectric performance of bentonite-based nanocomposites.

1. INTRODUCTION

In recent years, polymer-clay nanocomposites have gained significant attention in both academic research and industrial applications due to their enhanced mechanical, thermal, and dielectric properties [1]. These materials were first investigated at Toyota Research Center, where they demonstrated higher strength, hardness, and thermal stability compared to conventional polymers [2]. Various preparation methods and modification techniques have been extensively explored to optimize their performance across different applications [3-5].

Bentonite, a layered silicate from the smectite group, is widely used in the synthesis of polymer-clay nanocomposites due to its chemical and physical properties. It consists of layers approximately 1 nm thick, separated by regular Van der Waals gaps [6]. Its unique structure allows for intercalation and exfoliation, making it a preferred choice for enhancing the functional properties of polymer matrices. Polyvinyl chloride (PVC) is a widely used commercial plastic due to its low cost and versatility. PVC-bentonite composites have been synthesized using solution mixing, suspension polymerization, and emulsion polymerization,

---

* e-mail: ugurk@kocael.edu.tr

and their dielectric properties have been studied extensively [7]. These composites exhibit high dielectric constants and low energy losses (tan δ), making them attractive for electrical insulation applications.

Several studies have demonstrated that the incorporation of nano-fillers, such as clay, into PVC matrices enhances dielectric properties. Research indicates that at low frequencies, these nanocomposites exhibit higher dielectric permittivity and lower energy loss compared to pristine PVC [8, 9]. Furthermore, modified montmorillonite-based PVC composites show improved exfoliation and dielectric stability due to enhanced polymer-clay surface interactions [10]. The incorporation of ZnO and clay nanoparticles has also been found to significantly enhance both thermal and dielectric properties, improving current-carrying capacity in energy transmission cables [11]. These findings position PVC-based clay nanocomposites as strong candidates for energy insulation systems [8-11].

Unlike conventional nanocomposites where clay is introduced as a filler into polymer matrices, the present study adopts a reverse design approach. Here, pristine bentonite functions as the primary dielectric phase, while small amounts of PVC are incorporated to modulate the surface charge environment. In this architecture, the polymer acts not as a dielectric carrier, but as a surface-adsorbed dipolar restrictor, intended to suppress excessive dipolar orientation and electrode polarization arising from the hydroxyl-rich clay surfaces. This controlled interaction aims to regulate the interfacial polarization mechanisms without relying on costly surface modifications, offering a low-cost, physically robust alternative to organically modified clay systems.

Beyond their dielectric performance, clay-polymer nanocomposites play a crucial role in polarization mechanisms. Their intercalation and exfoliation structures contribute to interfacial interactions, which influence dielectric constant variations [6]. Mechanisms such as Maxwell-Wagner-Sillars (MWS) polarization and ionic polarization govern their dielectric behavior. In particular, clay additives suppress electrode polarization at low frequencies, minimizing energy loss, while at high frequencies, they maintain polarization stability. It has been reported that Na-bentonite composites in a PVA matrix exhibit limited intercalation, yet even this limited interaction reduces segmental polarization, leading to a lower dielectric constant [12]. This suppression of electrode polarization enhances their potential for microelectronic applications.

While many studies focus on modified clay–polymer systems, investigations involving pristine bentonite and its interaction with small amounts of polymer remain limited. This study aims to bridge this gap by conducting a detailed investigation of the dielectric properties of PVC–pristine bentonite nanocomposites, providing insight into their polarization mechanisms and assessing their potential for energy insulation and electronic applications.

2. MATERIAL METHOD

2.1. Materials and Preparation

Pristine bentonite, with a cation exchange capacity (CEC) of 85 meq/100 g, was supplied by Eczacıbaşı Esan A.Ş. (Istanbul, Türkiye). Polyvinyl chloride (PVC) was purchased from Aldrich, and chloroform (used as a solvent) was obtained from Fluka.

Predetermined amounts of PVC (25, 35, 60, 75, and 100 mg) were dissolved in 50 mL of chloroform, followed by the addition of 1 g of pristine bentonite to the solution. The mixtures were stirred at room temperature (RT) at 120 rpm for 8 hours. After stirring, the suspensions were filtered, and the obtained solid samples were dried at room temperature for 24 hours.

2.2. Characterization of Materials

The chemical composition of pristine bentonite was determined using X-ray fluorescence spectrometry (XRF, Bruker S8 Tiger). The chemical composition of pristine bentonite is presented in Table 1. The Fourier Transform Infrared (FT-IR) spectra of pristine bentonite and pristine bentonite-PVC composites were recorded using a Shimadzu 8201/86601 PC Infrared spectrometer. Measurements were conducted in the 400–4000 cm^{-1} wavelength range with a 1 cm^{-1} spectral resolution. For sample preparation, 10 mg of the material was mixed with 500 mg of KBr. The mixture was homogenized in a mortar, and 200 mg of the homogenized powder was compressed under a 6-ton pressure to form FT-IR pellets.

The X-ray diffraction (XRD) patterns of pristine clay and composites were obtained using a Rigaku X-ray diffractometer with Cu-Kα radiation (λ = 1.54 Å). Scans were conducted in the 2θ range of 2°–26° with a resolution of 0.02° 2θ.

For dielectric measurements, the samples were pressed into 13 mm diameter discs (pellets) under a 6-ton hydraulic press. Dielectric properties were analyzed at room temperature using a Novo Control Alpha-A high-resolution dielectric, conductivity, and impedance analyzer over the frequency range of 1 Hz to 10 MHz. A schematic representation of the dielectric measurement setup is shown in Figure 1, illustrating the configuration of the gold-plated electrodes, disc-shaped sample geometry, vacuum chamber, and the connection to the NovoControl analyzer. The pellet samples used for dielectric measurements had a diameter of 13 mm and a thickness in the range of 0.90–1.00 mm. However, as the gold-plated electrodes used in the NovoControl system have a diameter of 1 mm, the actual contact area during measurement was 0.00785 cm^2.

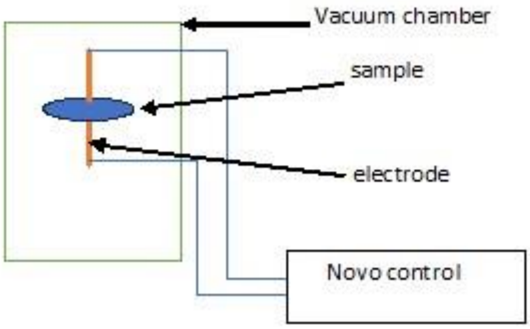

Figure 1. *Schematic representation of the dielectric measurement system. A 13 mm diameter disc-shaped sample (~0.9–1 mm thickness) is sandwiched between two 1 mm diameter gold-plated electrodes inside a vacuum-sealed measurement chamber with temperature control*

In dielectric measurements, the complex permittivity of a material is expressed in terms of its real and imaginary components. The real part (ε′) represents the material's ability to store electric energy (i.e., dielectric polarization), whereas the imaginary part (ε″) reflects the energy dissipation or dielectric loss under an alternating electric field. The loss tangent (tan δ), defined as the ratio ε″/ε′, is commonly referred to as the dielectric loss factor and quantifies the inefficiency of polarization.

The AC conductivity (σ_{ac}) describes frequency-dependent charge transport and is directly related to dielectric loss. These parameters were calculated using the following equations:

$$\varepsilon' = C_p/C_0 \tag{1}$$

$$\varepsilon'' = \varepsilon' \tan\delta \tag{2}$$

$$\sigma_{ac} = 2\pi f \varepsilon_0 \varepsilon'' \tag{3}$$

where;
ε′: real part of permittivity (dielectric polarization capacity),
ε″: imaginary part of permittivity (dielectric loss),
tan δ: dielectric loss factor (ε″/ε′),
σ_{ac}: AC conductivity (frequency-dependent conductivity),

f: frequency (Hz),
ε_o: permittivity of free space (8.85×10^{-12} F/m),
C_p: measured capacitance,
C_o: vacuum capacitance.

Table 1. *The chemical composition of pristine bentonite*

Oxide	Concentration (%)
SiO_2	79.9
Al_2O_3	13.1
Fe_2O_3	0.78
TiO_2	-
CaO	1.61
MgO	2.92
Na_2O	0.31
K_2O	0.82
L.O.I. (Loss on Ignition)	0.56

3. THE RESEARCH FINDINGS AND DISCUSSION

The XRF results of pristine bentonite indicate that it has a typical aluminosilicate structure, characterized by high SiO_2 (79.9%) and Al_2O_3 (13.1%) content. The obtained chemical analysis results, along with the CEC value (85 meq/100 g), suggest that the bentonite has a balanced distribution of sodium and calcium ions due to its low Na_2O (0.31%) and CaO (1.61%) content. Therefore, it can be classified as a natural pristine bentonite exhibiting transitional characteristics between sodium and calcium bentonites.

The infrared spectra of the pristine bentonite are presented in Figure 2. The FTIR spectrum of pristine bentonite reveals characteristic vibrational bands associated with its mineral structure. A distinct peak observed at 3628 cm^{-1} corresponds to the stretching vibrations of structural hydroxyl groups. Additionally, peaks at 3445 cm^{-1} and 1647 cm^{-1} are attributed to the stretching and bending vibrations of adsorbed water molecules, respectively. The spectral region between 1030 and 1093 cm^{-1} represents the stretching vibrations of Si–O bonds within the silicate structure, typically appearing as sharp and occasionally split peaks. The bending vibrations of OH groups at 916 cm^{-1} are associated with dioctahedral 2:1 layered silicates. The peak observed at 844 cm^{-1} corresponds to Al–Mg–OH vibrations. Peaks at 667 cm^{-1} and 629 cm^{-1} represent the bending vibrations of Si–O–Si linkages characteristic of the silicate framework. The lower-frequency bands at 519 cm^{-1} and 470 cm^{-1} are attributed to Si–O deformation and amorphous silica, respectively. Finally, the peak at 418 cm^{-1} corresponds to the deformation vibrations of oxygen atoms bonded to Mg or Al. These results are consistent with findings reported in previous studies. The vibrational modes of adsorbed water and silicate structures are in agreement with the findings of previous studies [13,14]. The spectral characteristics clearly reveal the dioctahedral structure of bentonite and the presence of hydroxyl and silicate vibrations.

The structural water vibration band of bentonite is typically observed in FTIR analyses at 3628 and 3618 cm^{-1}. These bands correspond to the vibrations of –OH groups present in the clay structure. The observed shifts in the structural water vibration bands in the FTIR spectra indicate that PVC interacts not only with the clay surface but also partially intercalates between the clay layers (Figure 3a). These findings align with the increase in basal spacing observed in XRD results, confirming that the polymer penetrates the interlayer regions and induces structural modifications in the clay matrix. Previous studies have demonstrated that changes in interlayer spacing and modifications in surface charge density can influence the frequency of these bands in similar systems [15,16].

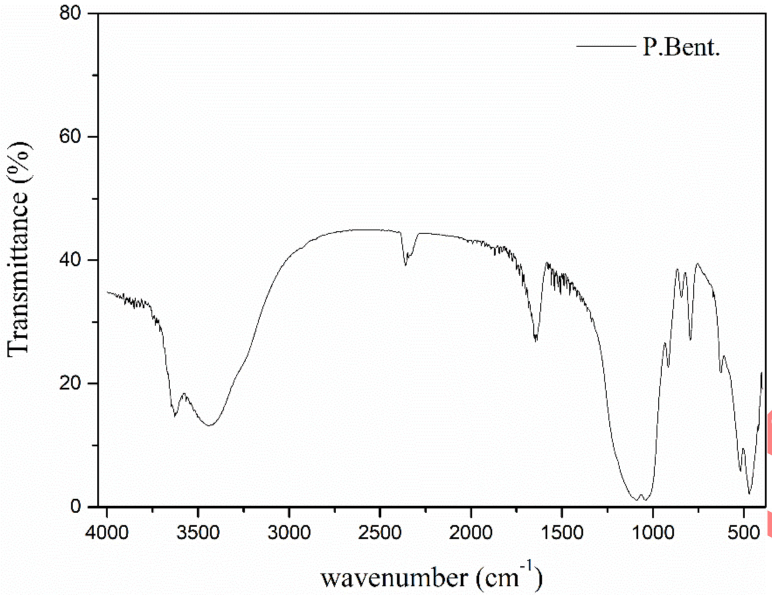

Figure 2. *The infrared spectra of the pristine bentonite*

The effect of PVC on structural water is associated with changes in surface charge density due to polymer adsorption. This phenomenon is observed in the FTIR analysis as a weakening and shift of the structural water bands. In particular, the interaction between the polar groups of PVC and –OH groups in the clay structure alters the interlayer spacing of bentonite. This finding is further supported by XRD analyses, which confirm the influence of PVC on basal plane expansion [12].

These results are crucial for understanding the effects of surface modifications and intercalation mechanisms on the structural water vibration bands. In conclusion, the observed shifts in the structural water vibration bands due to PVC loading can be evaluated in the context of the intercalation process and surface-polymer interactions. The confirmation of intercalation through XRD analysis provides a broader interpretation of the FTIR findings, reinforcing the structural modifications induced by PVC incorporation [17]. The infrared (IR) vibrational bands corresponding to adsorbed water molecules on the bentonite surface were observed at 3445 cm^{-1} (stretching vibration) and 1647 cm^{-1} (bending vibration). Upon PVC loading, shifts in these bands were detected. Specifically, the 3445 cm^{-1} band shifted to 3390 cm^{-1} after PVC incorporation and to 3382 cm^{-1} for low-mass PVC loadings (≤50 mg). Similarly, the bending vibration band at 1647 cm^{-1} shifted to 1633 cm^{-1} with PVC addition.

These shifts indicate that the adsorbed water molecules interact with polymer molecules, leading to modifications in the surface charge distribution of the bentonite. The shift in surface water vibrational bands in bentonite-PVC composites provides crucial insights into polymer-clay interactions. In pristine bentonite, the stretching vibration band of adsorbed water was observed at 3445 cm^{-1}. Upon PVC incorporation, this band shifted to 3390 cm^{-1}, and for lower PVC loadings, it further shifted to 3382 cm^{-1}. This suggests that PVC molecules form hydrogen bonds with the clay surface. These spectral shifts are primarily attributed to hydrogen bonding interactions between the polar chlorine (Cl) groups in PVC and the hydroxyl (OH) groups on the clay surface.

Similarly, a shift in the bending vibration band of water from 1647 cm^{-1} to 1633 cm^{-1} was detected, further supporting the influence of hydrogen bonding (Figure 3b). Research has shown that hydrogen bonding influences FTIR spectra by shifting band frequencies to lower wavenumbers, providing insights into bond strength [18]. It has been reported that as the strength of hydrogen bonds increases, the frequency shift becomes more pronounced [19]. Additionally, in FTIR analyses, along with such shifts, XRD results also play a crucial role in understanding the structural effects of surface-polymer interactions. The detection of changes in basal plane spacing via XRD can determine whether intercalation has occurred and support FTIR findings. In this context, it can be stated that the Cl groups of PVC form strong hydrogen bonds with the OH groups on the clay surface, resulting in the observed band shifts.

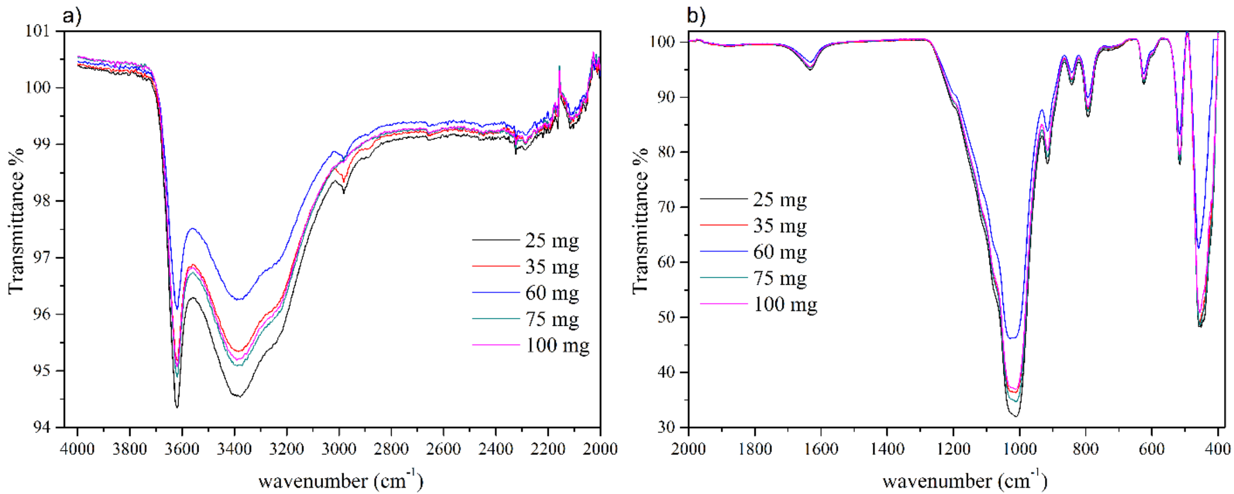

Figure 3. *The infrared spectra of the pristine bentonite-PVC nanocomposites a)4000-2000 cm^{-1} b)2000-400 cm^{-1}*

At low PVC loadings, these bands were prominent, whereas at high PVC loadings, they weakened and exhibited shoulder behavior. This suggests that polymer chains establish strong interactions with the clay surface. Van der Waals interactions, particularly in the structure where CH_3 groups come into contact with the surface, can lead to weakened and shifted vibrations The shift of this band to 2908 cm^{-1} at low PVC loadings may reflect weak polar interactions of CH_2 groups with the clay surface. This shift indicates the influence of Van der Waals interactions and the impact of surface charge distribution on the structural arrangement of PVC chains [15-17]. The shoulder behavior and broadening of vibrational bands suggest that PVC's molecular chains interact strongly enough with the clay surface to disrupt structural order. The variations observed in the vibrational bands of CH_3 and CH_2 groups further support the effect of polymer chain alignment on the clay surface [12].

Low-intensity bands around 2100, 1990, and 1870 cm^{-1} were observed. The absence of these bands in pristine bentonite suggests that they may be associated with impurities or by-products formed during PVC production. In the literature, vibrational modes in these wavenumber regions have been attributed to additives such as thermal stabilizers, plasticizers, or carbonyl groups used in PVC manufacturing [20]. Additionally, these bands may also originate from combination modes that occur during PVC processing [21].

Changes observed in the Si–O vibration bands of composites provide valuable insights into the structural properties of the clay and the polymer–surface interactions. In bentonite, the Si–O vibration band typically observed around 1030 cm^{-1} shifts in the presence of polymer, especially at lower PVC loadings. Additionally, a secondary band around 1011 cm^{-1} exhibits shoulder-like behavior. These spectral changes can be attributed to polar interactions formed between PVC molecules and the bentonite surface. Hydrogen bonding or variations in surface polarity could affect the local bonding environment of Si–O groups, causing these shifts [22]. The attenuation observed at 1093 cm^{-1} is thought to result from structural irregularities in the amorphous silica network. The polar characteristics of chlorine atoms in PVC can induce changes in the surface polarity of the clay, directly influencing the Si–O vibrational frequencies. Additionally, more pronounced shifts observed with lower PVC loadings highlight the role of PVC's molecular size in the strength of these interactions.

The changes observed in the Si–O vibration bands in composites provide important information about the structural properties of the clay and its interactions with the polymer surface. In literature, polymer–clay interaction studies supported by XRD analyses have explained the structural effects of surface modifications [17]. The XRD data help clarify the interlayer structural changes resulting from these interactions.

Weak vibrational bands were observed at around 743 and 692 cm^{-1} in composites containing PVC, which are attributed to C–Cl stretching vibrations of PVC [23]. The absence of these bands in pristine bentonite suggests their emergence due to PVC incorporation. These findings imply that interactions between PVC molecules and bentonite surfaces, potentially via Van der Waals forces or hydrogen bonds, influence the vibrational frequencies of C–Cl groups.

The shifts and attenuations observed in Si–O vibrational bands (1030–1093 cm^{-1}) indicate that chlorine atoms in PVC alter surface polarity, affecting the local bonding environments of Si–O groups. Additionally, the emergence of new bands around 743 and 733 cm^{-1} suggests specific interactions between the C–Cl groups of PVC and the bentonite surface. Moreover, the weakening and shifting of CH_2 and CH_3 vibrational bands observed between 2920–2982 cm^{-1} indicate the polymer chains' arrangement through Van der Waals interactions with the surface.

Supporting these findings with XRD analyses provides critical insights into understanding the interaction mechanisms at PVC-bentonite composite surfaces. In particular, the effects of surface polarity and intercalation processes on the shifts observed in FTIR analyses play a critical role in the design of polymer–clay composites. At lower PVC loadings ($\leq$50 mg), hydrogen bonding effects become more pronounced, resulting in larger frequency shifts in adsorbed water bands. However, at higher PVC loadings, changes in interlayer charge distribution accompany surface interactions, reducing their strength.

Figure 4 (a) (2-26°) and (b) (5.2-6.6°) show XRD spectra of pristine bentonite and pristine bentonite/PVC nanocomposites. The characteristic X-ray diffraction (XRD) patterns of pristine bentonite exhibit distinct peaks revealing the mineral's structural features. Typical basal plane spacings (d_{001}) of bentonite were detected at 2θ values of 6.12° (d001=1.444 nm), 17.9° (d_{002}=0.495 nm), 20.1° (0.441 nm), and 22.2° (0.400 nm). These values indicate the layered structure of bentonite, providing insights into the crystallographic arrangement of clay minerals. The peak observed at 17.9° (d ~ 0.495 nm) generally corresponds to the second-order basal plane (002) in the smectite structure or surface adsorption phenomena. The peak at 20.1° (d ~ 0.441 nm) may originate from reflections associated with tetrahedral sheets in the silicate structure, often indicative of the presence of amorphous silica.

The peak observed at 22.2° (d ~ 0.4 nm) indicates other regular reflections in the tetrahedral or octahedral layer structure of bentonite. It is an indicator of more compact and orderly structures. These characteristics of bentonite form a fundamental reference point for evaluating the effects of processes such as surface modifications or polymer loadings.

As anticipated, the broad peak observed around 12.8° in the XRD patterns clearly indicates the semi-crystalline nature of PVC. This peak is consistent with literature reports and is typically attributed to the coexistence of amorphous and semi-crystalline regions within polyvinyl chloride. Highlighting this observation with relevant literature references strengthens the structural interpretation of polymer–clay composites and helps clarify interactions between polymer chains and clay surfaces [23].

In the literature, numerous studies based on the XRD analysis of bentonite have demonstrated that changes in the basal plane distances of clay layers are associated with polymer loadings and surface interactions. For instance, it was) emphasized that polymer-clay surface interactions can alter interlayer distances, leading to significant changes in structural regularity [6,16]. These changes typically arise from the intercalation of the polymer into the clay layers or its adsorption onto the clay surface. However, even in cases where no expansion of the basal plane (d_{001}) occurs i.e., when intercalation is not observed the interaction of additives with the clay surface can still cause changes in surface charge density, resulting in a slight contraction of the basal plane distance [6].

The Table 2 shows the basal plane (d_{001}) reflection angles (2θ) and corresponding d-spacing values for raw bentonite and its composites with varying PVC loadings. The increase in d-spacing for PVC-loaded composites compared to raw bentonite suggests intercalation of PVC into the interlayer galleries of bentonite, consistent with structural reorganization due to polymer-clay interactions. The slight fluctuations in d-spacing at higher PVC loadings (e.g., 75 mg and 100 mg) may indicate partial intercalation or surface adsorption rather than complete exfoliation.

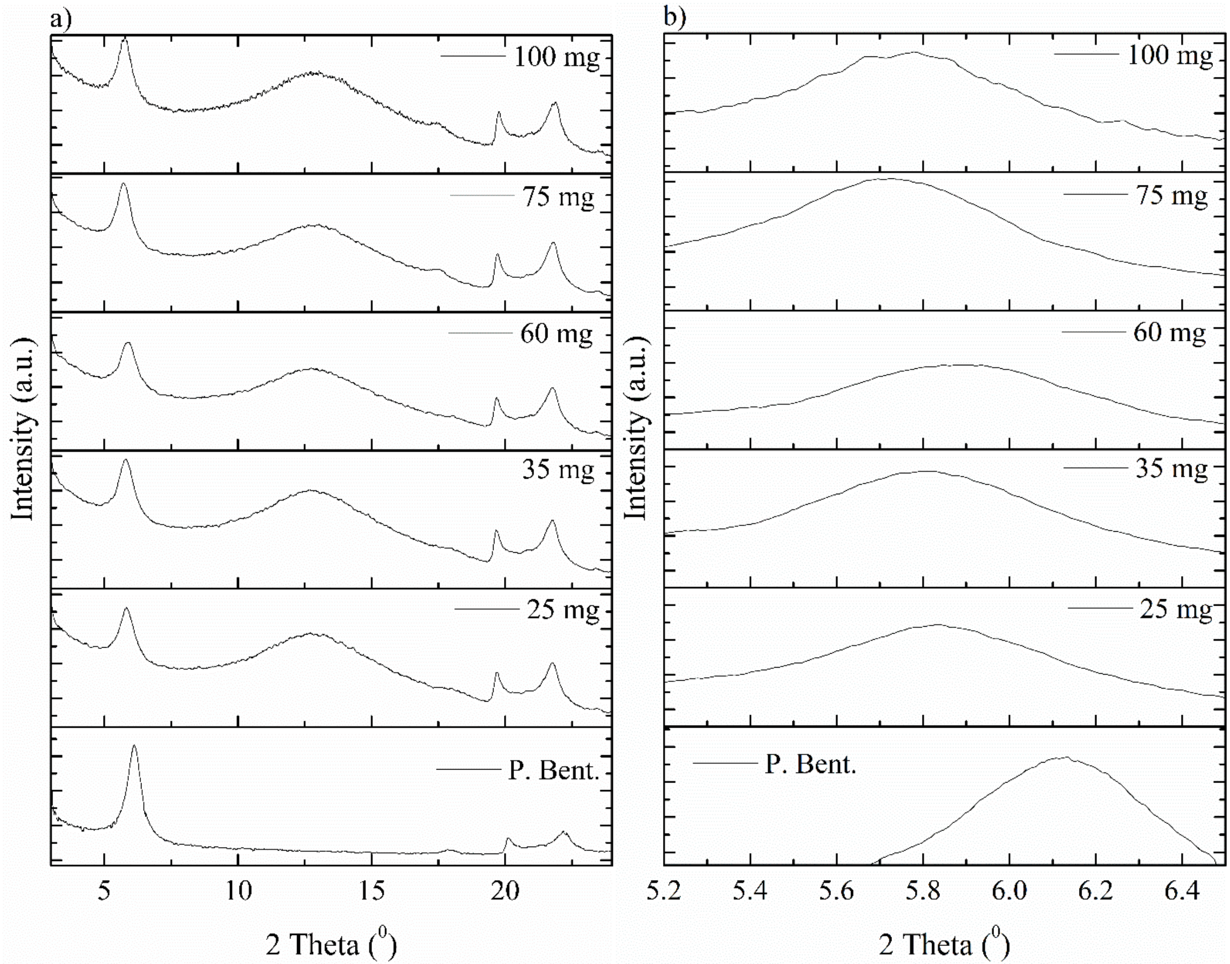

Figure 4. *XRD spectra of the pristine bentonite-PVC nanocomposites a)2-26 ° b)5.2-6.6 °*

Table 2. *Basal plane (d_{001}) reflection angles (2θ) and corresponding d-spacing values for pristine bentonite and its composites with varying PVC loadings*

Sample	2-Theta(°)	d-spacing (d_{001}) (nm)
pristine bentonite	6.12	1.444
25 mg	5.82	1.518
35 mg	5.80	1.521
60 mg	5.89	1.506
75 mg	5.74	1.538
100 mg	5.76	1.535

Smectite-type layered silicates, such as bentonite, are generally considered unfavorable for polymer intercalation without surface modifications. However, under specific conditions, polar polymers like PVC can effectively adhere to the clay surface, initiating intercalation or surface interactions. It was emphasized that structural modifications of smectites facilitate the entry of polymers into interlayer spaces [2]. It was also demonstrated that exfoliation in polymer nanocomposites provides superior mechanical and thermal properties. The intercalation of polymer molecules into clay layers is typically influenced by factors such as surface charge density and polarity [24].

This phenomenon has been linked to the barrier properties of nanocomposites and explained in terms of structural effects caused by changes in surface charge density [25,26]. The intercalation of PVC into bentonite interlayers arises not only from physical loading but also from strong interactions between the surface energy, the natural structure of the clay, and the polar groups of the polymer. These results confirm that polymer-clay surface interactions reported in the literature are also valid in the context of PVC-bentonite composites, and these interactions are concretely observed through changes in basal plane distances. However, the results from infrared studies on structural water vibrations have now gained greater significance.

The changes in structural water vibration bands can be explained by the intercalation of PVC into the clay layers. The weakening of the 3628 cm⁻¹ band and its shift to 3618 cm⁻¹ in FTIR are interpreted as a result of the intercalation process and surface interactions, supported by XRD analyses. The increase in basal plane width observed in XRD results indicates that polymer molecules have penetrated between the clay layers, altering the structural order of the clay. This mechanism reveals that intercalation is not merely a physical displacement but also involves chemical effects associated with hydrogen bonding and changes in surface charge density. In conclusion, the combined evaluation of FTIR and XRD enables a comprehensive understanding of polymer-clay interactions in PVC-bentonite composites.

Figure 5 shows permittivity values of pristine bentonite (inset) and pristine bentonite/PVC nanocomposites. The high permittivity values observed in the low-frequency region for PVC-loaded bentonite nanocomposites can be attributed to the electrode polarization effect. Electrode polarization is a mechanism that arises from the accumulation of charge carriers at the electrode surfaces and is particularly prominent in heterogeneous and multiphase materials. However, as the PVC loading increases, the electrode polarization effect decreases, and this situation exhibits a distinct trend, especially in nanocomposites containing 35 mg and 100 mg of PVC.

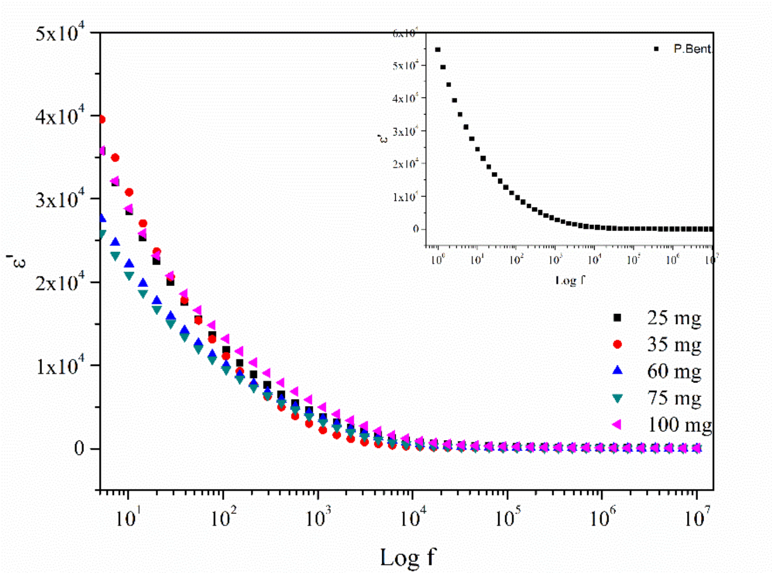

***Figure 5.** Frequency-dependent permittivity (ε') variations of pristine bentonite and its nanocomposites*

In samples with low PVC content (25 mg and 60 mg PVC-loaded composites), permittivity values remain at relatively low levels due to the limitation of electrode polarization. However, in the composite containing 35 mg PVC, a more pronounced decrease is observed starting from 80 Hz. This indicates that the polymer strongly interacts with the clay surface, restricting the movement of surface charge carriers and weakening electrode polarization. On the other hand, the increase in permittivity observed in the composite loaded with 100 mg PVC suggests that high polymer loading may have increased the mobility of charge carriers within the system, making the accumulation at the electrode surfaces more prominent again.

These results demonstrate that the interaction of PVC with the clay surface and interlayer regions directly affects the dielectric properties of the system. At this point, the findings from XRD and FTIR analyses must be examined to discuss in greater detail the distribution of PVC within the clay matrix and its effect on charge transport mechanisms. Electrode polarization occurs due to the accumulation of charge carriers at the electrode surfaces under the influence of an electric field and is commonly observed in multiphase and heterogeneous systems.

The XRD results revealed that PVC undergoes partial intercalation into the interlayer galleries of bentonite, leading to an expansion in basal plane widths. This intercalation likely induces the localization of charge carriers in distinct regions within the clay's internal structure and on its surface, directly modulating electrode polarization. Notably, in the composite with 100 mg PVC loading, the basal plane expansion became more pronounced, while FTIR analysis detected significant shifts in structural water vibration bands. These observations suggest that alterations in the clay's hydration state and surface charge distribution actively contribute to polarization mechanisms in the low-frequency regime. The correlation between PVC's intercalation dynamics and charge carrier distribution may explain the re-emergence of electrode polarization at higher PVC concentrations.

In the literature, high permittivity values observed in the low-frequency region of clay-based polymer composites have been attributed to the accumulation of charge carriers at electrode surfaces [12]. Electrode polarization can become more pronounced due to the contribution of water molecules on the clay surface to charge transport capacity. Water molecules on the clay surface may enhance the electrode polarization effect, leading to higher permittivity values in the low-frequency region. However, the interaction of PVC with the clay surface can restrict the mobility of surface water, thereby reducing the electrode polarization effect [6]. In this study, higher permittivity values were observed at low frequencies for composites with 35 mg and 100 mg PVC loadings compared to other composites. This suggests that partial intercalation into the clay layers may have occurred in the 100 mg PVC-loaded composite, contributing to electrode polarization and thereby increasing permittivity again. The adsorption of PVC onto the clay surface and its partial intercalation, along with changes in surface charge distribution, may have influenced the interfacial polarization (MWS) mechanism, leading to a reduction in permittivity at specific PVC loadings [10]. Notably, the significant decrease observed in the composite loaded with 35 mg PVC indicates that PVC binds more strongly to the clay surface, limiting interfacial charge accumulation and thereby restricting the high permittivity effect observed at low frequencies. In conclusion, the clay-polymer interactions reported in the literature are consistent with our dielectric findings and provide critical data on how PVC loading affects electrode polarization.

The changes observed in permittivity values in the mid-frequency range (~10^3–10^6 Hz) indicate that the interfacial polarization (MWS) mechanism becomes dominant in PVC-bentonite nanocomposites. In this frequency range, interactions between the polymer and the clay surface/interlayer regions lead to the accumulation of charge carriers at clay-polymer interfaces, resulting in distinct charge separation (MWS). In this frequency range, permittivity values are lower for composites with low PVC loadings (25 mg and 35 mg) but become more pronounced as the PVC loading increases (60 mg, 75 mg, and 100 mg). The rapid decrease in permittivity observed in the composite containing 35 mg PVC in the low-frequency region persists into the mid-frequency region, resulting in this composite exhibiting the lowest permittivity values compared to other composites. This suggests that PVC forms a strong bond with the clay surface, limiting interfacial charge accumulation. Conversely, in the composite loaded with 100 mg PVC, the interfacial polarization effect increases again, likely due to the polymer chains adopting a more irregular distribution within the clay layers, leading to localized accumulation of charge carriers.

In clay-polymer composites, interfacial polarization has been reported to depend on the strength of polymer-surface interactions and the clay's inherent surface charge density [12] PVC's high polarity and chlorine-containing groups, which form hydrogen bonds with the clay surface, may restrict the movement of charge carriers and suppress interfacial charge separation [10] These results indicate that PVC loading not only affects electrode polarization but also influences interfacial charge accumulation, demonstrating that PVC-clay interactions directly govern the dielectric behavior of the system.

In the high-frequency region (~10^6 Hz and above), the permittivity values of PVC-bentonite composites decrease significantly and approach similar levels across all samples. This indicates that charge transport mechanisms such as electrode polarization and interfacial polarization, which dominate at low frequencies, become ineffective, and the system responds based solely on electronic polarization and ionic polarization.

Figure 6 presents the frequency-dependent dielectric loss (ε'') variations of raw bentonite and its nanocomposites. A decrease in dielectric loss values is observed as the frequency increases. This behavior is associated with the reduced mobility of charge carriers in dielectric materials at high frequencies. The high dielectric loss values in the low-frequency region (<1 kHz) indicate the effectiveness of mechanisms such as electrode polarization and surface charge accumulation. Notably, a significant increase in loss is observed in the low-frequency region for nanocomposites loaded with 25 mg, 35 mg, and 100 mg PVC compared to raw bentonite. This suggests that the polymer interacts with the clay surface and interlayer regions, influencing the movement of charge carriers. The changes in basal plane distances induced by PVC (observed in XRD results) and the shifts in structural water and Si-O vibration bands (detected in FTIR analysis) structurally corroborate these interactions. As the frequency increases, the effect of electrode polarization diminishes, and dielectric loss values decrease. In this region, interfacial polarization (MWS) becomes prominent, and the loss mechanism differentiates due to the localization of charge carriers at the clay-polymer interface. The reduction in loss observed around 1 kHz in the composite loaded with 35 mg PVC indicates that the polymer exhibits a strong interaction with the clay surface, restricting the movement of charge carriers.

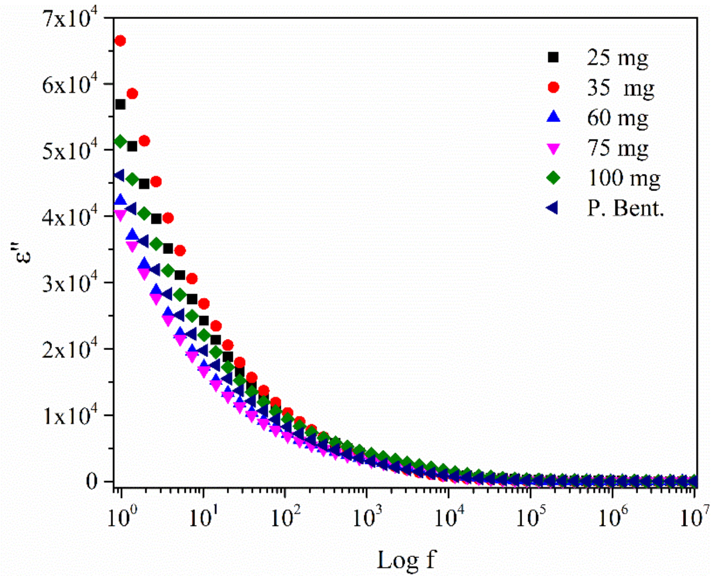

Figure 6. *Frequency-dependent dielectric loss (ε'') variations of pristine bentonite and its nanocomposites*

The effect of PVC’s polar side groups on dielectric loss becomes particularly prominent in low and medium frequency regions. Due to its polar chlorine (Cl) groups, PVC forms hydrogen bonds and dipole-dipole interactions with the clay surface, directly influencing charge transport mechanisms [27]. In the low-frequency region, interaction of PVC molecules with the clay surface determines the strength of electrode polarization, while in the mid-frequency region, MWS interfacial polarization becomes dominant [8] Notably, at high PVC loadings (100 mg), the polymer causes increased charge accumulation on the clay surface, leading to elevated dielectric loss. The intercalation of PVC into the clay matrix alters the layer charge density, which in turn modifies the mobility of charge carriers and the dielectric loss mechanism [28]). These findings from the literature support the PVC loading-dependent changes in dielectric loss values observed in this study and highlight the critical role of polar PVC groups in modulating dielectric properties through interactions with the clay surface.

Figure 7 shows the frequency-dependent loss factor (tanδ) variations of pristine bentonite and nanocomposites. The relaxation frequency shifts observed in bentonite-PVC nanocomposites can be attributed to changes in charge transport dynamics due to interactions between the clay and polymer. The relaxation frequency of raw bentonite, determined as 39 kHz, shifted to lower frequencies after PVC incorporation. Specifically, the relaxation frequency decreased to 12 kHz in the nanocomposite with 35 mg PVC, while it was measured as 17 kHz for the 25 mg PVC-loaded composite. For the 60 mg PVC-loaded system, the relaxation frequency increased to 24 kHz, dropped back to 17 kHz at 75 mg PVC loading, and reverted to 24 kHz again at 100 mg PVC loading.

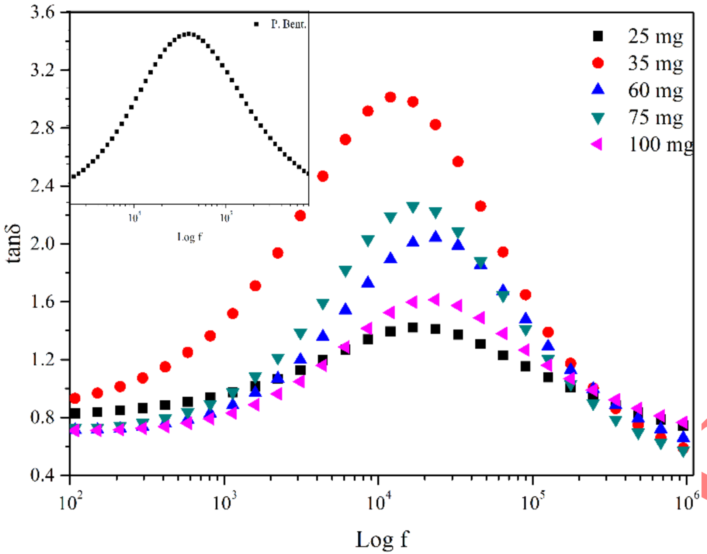

Figure 7. *Frequency-dependent loss factor (tan δ) variations of pristine bentonite and nanocomposites*

It was demonstrated that the intercalation of polymer into the clay matrix reduces interlayer ion mobility, which lowers the relaxation frequency and allows low-frequency polarization mechanisms to dominate. It was also emphasized that changes in surface charge distribution in polymer-clay composites can lead to significant shifts in relaxation frequencies [2]. It was reported that alterations in surface charge density directly influence dipole orientation, causing frequency shifts in dielectric responses [26]. Another mechanism explaining the relaxation frequency shifts caused by PVC loading is dipole mobility resulting from polymer-surface interactions. It was demonstrated that changes in surface charge density during clay-polymer interactions directly influence dipole orientation, leading to significant shifts in relaxation frequency [26].

The increase in relaxation frequency to 24 kHz in the 100 mg PVC-loaded composite indicates reduced interactions between the high polymer content and the clay surface, suggesting the polymer has reached a certain saturation point. As noted in previous studies, high polymer loadings can cause polymer chains to self-agglomerate rather than interact homogeneously with the clay surface, leading to irregular surface structures. This irregularity increases dipole mobility, enabling the relaxation frequency to shift back to relatively higher values [6,12].

In conclusion, the relaxation frequency shifts observed in PVC-loaded nanocomposites are shaped by both polymer-clay surface interactions and the mobility of charge carriers. XRD and FTIR data provide critical evidence supporting these mechanisms, demonstrating that PVC's binding to the clay surface via polar groups significantly alters dielectric relaxation properties. Similar studies in the literature corroborate the dominance of these mechanisms in clay-polymer systems, aligning with and reinforcing the findings of this work.

To support the dielectric observations, frequency-dependent AC conductivity (σ_{ac}) values were also evaluated. The σ_{ac} plots revealed a typical dispersion pattern remaining nearly constant at low frequencies and increasing at higher frequencies (Figure 8). This behavior is indicative of interfacial polarization and is consistent with Maxwell–Wagner–Sillars (MWS) type relaxation.

In particular, composites with intermediate PVC loading (35–75 mg) exhibited significantly lower σ_{ac} values across the frequency range compared to the 25 mg and 100 mg systems. This reduction is attributed to stronger polymer–clay surface interactions that suppress dipole mobility and limit charge carrier transport. Similar suppression effects were reported in PMMA–bentonite nanocomposites, where intercalation and water removal reduced ion mobility and dielectric relaxation, resulting in lower σ_{ac} and permittivity values [6].

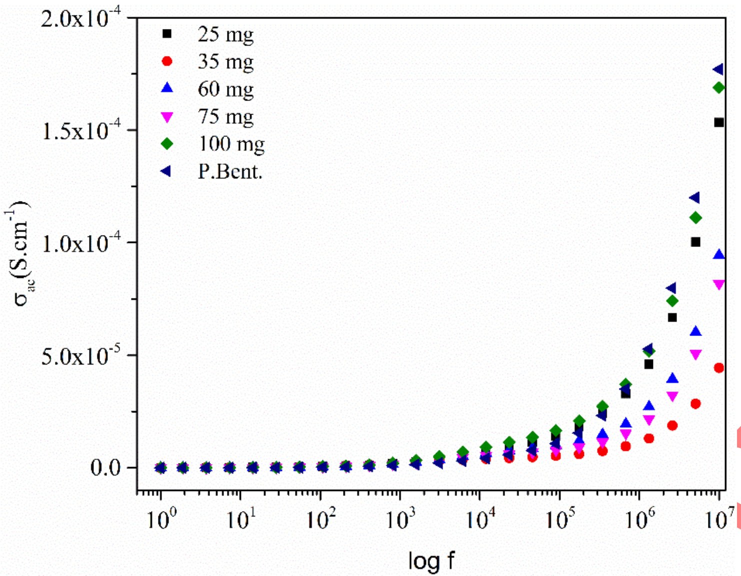

***Figure 8.** Semi-log plot of AC conductivity (σ_{ac}) vs frequency for bentonite–PVC composites*

Additionally, it was demonstrated that PVA adsorption on bentonite surfaces effectively suppressed electrode polarization and reduced dielectric losses in PVA–bentonite composites. This behavior was attributed to restricted dipolar orientation of adsorbed water molecules and surface hydroxyl groups, which led to a stabilized dielectric response and reduced σ_{ac} at low frequencies [12].

These results align with recent findings in BE–PLA systems, where increasing bentonite content led to a plateau region in σ_{ac} at low frequencies, followed by a power-law increase at higher frequencies. This behavior was associated with filler-induced tunneling and interfacial polarization [29]. In contrast, in CPTES-modified bentonite systems, AC conductivity was reported to increase due to functional groups introducing additional charge carrier pathways [30].

AC conductivity (σ_{ac}) values were modeled using the simplified Jonscher power law equation, $\sigma_{ac}(f) = A \cdot f^n$, where f is the frequency in Hz, A is the pre-exponential factor, and n is the power law exponent representing the degree of frequency dispersion. The calculated A and n values for each composition are summarized in Table 3, and the variation of the power law exponent (n) with PVC content is presented in Figure 9. The pristine bentonite exhibited an n value of 0.60, indicating more frequency-dependent conduction, while the composites with 35–75 mg PVC showed reduced n values (as low as 0.39), reflecting suppressed dipolar motion and stronger interfacial polarization. Notably, a slight increase in n at 100 mg PVC loading suggests partial recovery of charge carrier mobility due to polymer oversaturation and reduced interaction with the clay surface. These trends further corroborate the earlier dielectric and conductivity observations, reinforcing the conclusion that the dielectric behavior in bentonite–PVC nanocomposites is modulated by surface interactions and polymer intercalation.

***Table 3.** Fitted parameters (A and n) from the Jonscher power law $\sigma_{ac}(f) = A \cdot f^n$ for pristine bentonite and PVC-loaded nanocomposites. The exponent n quantifies the frequency dependence of AC conductivity, and lower values indicate stronger confinement effects or limited dipolar relaxation*

Sample	A	n
25 mg	4.89×10^{-8}	0.5
35 mg	7.57×10^{-8}	0.39
60 mg	3.95×10^{-8}	0.49
75 mg	3.96×10^{-8}	0.47
100 mg	4.50×10^{-8}	0.52
0 (P.Bent)	6.95×10^{-9}	0.6

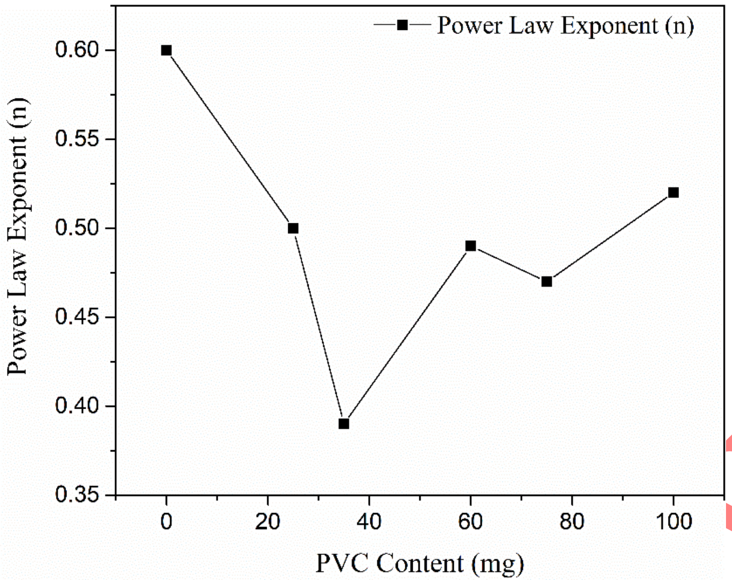

Figure 9. *Variation of the frequency exponent n (from the Jonscher power law) as a function of PVC content in the bentonite–PVC nanocomposites. The data point at 0 mg represents pristine bentonite without any polymer addition*

Taken together, these findings confirm that the observed suppression in σ_{ac} for PVC-loaded bentonite composites is governed by interfacial polarization and reduced charge mobility, rather than enhanced conduction pathways. Therefore, surface-adsorbed PVC acts as a dielectric barrier that limits conduction, in contrast to modified-clay systems where conductivity is intentionally enhanced.

4. RESULTS

In this study, the structural and dielectric properties of bentonite-PVC nanocomposites were investigated using X-ray Diffraction (XRD), Fourier Transform Infrared Spectroscopy (FTIR), X-ray Fluorescence Spectrometry (XRF), and Dielectric Spectroscopy (DS). The results demonstrated that PVC molecules were partially intercalated into the bentonite layers. The increase in basal plane spacing observed in XRD analyses supports the intercalation of PVC into the interlayer galleries. Additionally, shifts in structural water vibration bands detected by FTIR revealed that PVC interacted not only with the bentonite surface but also with the interlayer regions. These findings indicate that structural changes occurred at the nanoscale, confirming that the bentonite-PVC system can be classified as a nanocomposite.

Dielectric analyses revealed that the high permittivity (ε') values observed in the low-frequency region of the nanocomposites are linked to electrode polarization and interfacial polarization mechanisms. While increasing PVC loading caused a decreasing trend in permittivity values, these values rebounded in the composite containing 100 mg PVC. This behavior can be attributed to the polymer saturating on the bentonite surface and the subsequent increase in the mobility of charge carriers. Dielectric loss (ε") and loss factor (tan δ) analyses revealed that the relaxation frequency shifted to the low-frequency region with increasing PVC loading. Notably, in the 35 mg PVC-loaded nanocomposite, the relaxation frequency dropped to 12 kHz, which was determined to originate from stronger interfacial interactions and restricted dipole mobility.

This trend was further supported by frequency-dependent AC conductivity (σ_{ac}) measurements, which exhibited a typical dispersion behavior remaining nearly constant at low frequencies and increasing at higher frequencies. This trend confirms the presence of interfacial polarization mechanisms, consistent with the Maxwell–Wagner–Sillars (MWS) model. Notably, PVC-bentonite composites with moderate PVC loadings (35–75 mg) displayed markedly lower σ_{ac} values, indicating suppressed dipole mobility and reduced charge carrier transport. To quantitatively assess this behavior, the simplified Jonscher power law, was applied. The fitted exponent values (n) exhibited a non-monotonic trend with PVC content, with a minimum around 35 mg loading, reflecting enhanced interfacial confinement. These conductivity results, in conjunction with dielectric loss and permittivity trends, confirm that polymer–clay interactions predominantly govern the dielectric relaxation and conduction mechanisms in the bentonite–PVC system. These findings indicate that the structural and dielectric properties of bentonite–PVC composites are directly linked to intercalation, surface interactions, and charge carrier distribution. Beyond the fundamental material characterization, the results have significant implications for both industrial and scientific applications. The observed increase in dielectric permittivity at low frequencies, along with enhanced interfacial polarization mechanisms, suggests that these nanocomposites have strong potential in electrical insulation materials, low-loss dielectric capacitors, and EMI shielding applications.

Additionally, the controlled reduction of electrode polarization at lower PVC loadings makes these composites promising candidates for high-sensitivity dielectric sensors and microelectronic applications, particularly in RC circuit components where suppressed electrode polarization can help reduce signal delay and improve timing accuracy.

The observed polymer–clay interactions also contribute to improved mechanical and thermal stability, which could be beneficial in structural polymer reinforcements, flame-retardant materials, and engineering plastic formulations. Furthermore, the ability to tune dielectric properties through PVC loading and intercalation mechanisms paves the way for the development of recyclable and high-performance dielectric composites, particularly for next-generation energy transmission cables, flexible electronics, and environmentally sustainable materials. These findings align with ongoing research in polymer–clay systems and demonstrate that bentonite–PVC nanocomposites can serve as a versatile class of materials for advanced dielectric and functional applications.

CONFLICTS OF INTEREST

No conflict of interest was declared by the authors.

REFERENCES

[1] Alexandre, M., and Dubois, P., "Polymer-layered silicate nanocomposites: preparation, properties and uses of a new class of materials", Materials Science and Engineering, 28: 1-63, (2000). DOI: https://doi.org/10.1016/S0927-796X(00)00012-7

[2] Ray, S.S., and Okamoto, M., "Polymer/layered silicate nanocomposites: a review from preparation to processing", Progress in Polymer Science, 28: 1539–1641, (2003). DOI: https://doi.org/10.1016/j.progpolymsci.2003.08.002

[3] Sheng, N., "Multiscale Micromechanical Modeling of the Thermal/Mechanical Properties of Polymer/Clay Nanocomposites", Phd. Thesis, Massachusetts Institute of Technology, Massachusetts, 1-183, (2006)

[4] Wang, L., Wang, K., Chen, L., and Zhang, Y., "Preparation, morphology and thermal/mechanical properties of epoxy/nanoclay composite", Composites: Part A, 37: 1890–1896, (2006). DOI: https://doi.org/10.1016/j.compositesa.2005.12.020

[5] Bhatt, C., Swaroop, R., Arya, A., and Sharma, A.L., "Effect of nano-filler on the properties of polymer nanocomposite films of PEO/PAN complexed with NaPF6", Journal of Materials Science and Engineering B, 5: 11-12, (2015). DOI: https://doi.org/10.17265/2161-6221/2015.11-12.003

[6] Kaya, A.U., Guner, S., and Esmer, K., "Effects of solution mixing temperature on dielectric properties of PMMA/pristine bentonite nanocomposites", Journal of Applied Polymer Science, 131: 39907-39914, (2014). DOI: https://doi.org/10.1002/app.39907

[7] Mansur, H.S., Sadahira, C.M., Souza, A.N., and Mansur, A.P., "FTIR spectroscopy characterization of poly(vinyl alcohol) hydrogel with different hydrolysis degree and chemically crosslinked with

glutaraldehyde", Materials Science and Engineering C, 28: 539–548, (2008). DOI: https://doi.org/10.1016/j.msec.2007.10.088

[8] Mohamed, A.T., "Thermal experimental verification on effects of nanoparticles for enhancing electric and dielectric performance of polyvinyl chloride", Measurement, 89: 28–33, (2016). DOI: https://doi.org/10.1016/j.measurement.2016.04.002

[9] Rozik, N.N., Abd-El Messieh, L.L., and Abd-El Nour, K.N., "The effect of modified pluronic on the distribution of fillers in the polyvinyl chloride matrix", Journal of Applied Polymer Science, 115: 1732–1741, (2010). DOI: https://doi.org/10.1002/app.31217

[10] Silva, T.F., Soares, B.G., Ferreire, S.C., and Sebastian, L., "Silylated montmorillonite as nanofillers for plasticized PVC nanocomposites: Effect of the plasticizer", Applied Clay Science, 99: 93–99, (2014). DOI: https://doi.org/10.1016/j.clay.2014.06.017

[11] Gouda, O.E., Darwish, M.M.F., Thabet, A., Lehtonen, M., and Osman, G.F.A., "Enhancement of the underground cable current capacity by using nano-dielectrics", Energy Science and Engineering, 12: 3647–3662, (2024). DOI: https://doi.org/10.1002/ese3.1822

[12] Akar, Y., and Kaya, A.U., "Investigation of structural, thermal and dielectric properties of PVA/Na-Bentonite composites", Journal of the Faculty of Engineering and Architecture of Gazi University, 40: 287-295, (2025). DOI: https://doi.org/10.17341/gazimmfd.1401676

[13] Wilson, M.J., Clay Mineralogy: Spectroscopic and Chemical Determinative Methods, 1st ed., Springer, Dordrecht, (1994).

[14] Madejova, J., "FTIR techniques in clay mineral studies", Vibrational Spectroscopy, 31: 1–10, (2003). DOI: https://doi.org/10.1016/S0924-2031(02)00065-6

[15] Kumari, N., Mohan, C., and Negi, A., "An investigative study on the structural, thermal and mechanical properties of clay-based PVC polymer composite films", Polymers, 15: 1922-1937, (2023). DOI: https://doi.org/10.3390/polym15081922

[16] Erdem, M., Ortac, K., Erdem, B., and Turk, H., "Reaktif organobentonit katkilarin sert poliuretan kopugun bazi performans ozellikleri uzerine etkisi", Journal of the Faculty of Engineering and Architecture of Gazi University, 32: 1209-1219, (2017). DOI: https://doi.org/10.17341/gazimmfd.369543

[17] Shanmugharaj, A.M., Rhee, K.Y., and Ryu, S.H., "Influence of dispersing medium on grafting of aminopropyltriethoxysilane in swelling clay materials", Journal of Colloid and Interface Science, 298: 854–859, (2006). DOI: https://doi.org/10.1016/j.jcis.2005.12.049

[18] Chuajiw, W., Nakano, M., Takatori, K., Kojima, T., Wakimoto, Y., and Fukushima, Y., "Effects of amine, amine salt and amide on the behaviour of carbon dioxide absorption into calcium hydroxide suspension to precipitate calcium carbonate", Journal of Environmental Sciences, 25: 2507–2515, (2013). DOI: https://doi.org/10.1016/S1001-0742(12)60284-8

[19] Branca, C., D'Angelo, G., Crupi, C., Khouzami, K., Rifici, S., Ruello, G., and Wanderlingh, U., "Role of the OH and NH vibrational groups in polysaccharide nanocomposite interactions: A FTIR-ATR study on chitosan and chitosan/clay films", Polymer, 99: 614-622, (2016). DOI: https://doi.org/10.1016/j.polymer.2016.07.086

[20] Czako, E., Vymazal, Z., Volka, K., Stibor, I., and Stepek, J., "Effect of stabilizers in the thermal treatment of PVC-VI. An I.R. spectroscopic study of the stabilization of PVC with Ba and Cd

stearates", European Polymer Journal, 15: 81-85, (1979). DOI: https://doi.org/10.1016/0014-3057(79)90253-2

[21] Efimov, A.M., and Pogareva, V.G., "IR absorption spectra of vitreous silica and silicate glasses: The nature of bands in the 1300 to 5000 cm-1 region", Chemical Geology, 229: 198–217, (2006). DOI: https://doi.org/10.1016/j.chemgeo.2006.01.022

[22] Kotal, M., and Bhowmick, A.K., "Polymer nanocomposites from modified clays: Recent advances and challenges", Progress in Polymer Science, 51: 127–187, (2015). DOI: https://doi.org/10.1016/j.progpolymsci.2015.10.001

[23] Gong, F., Feng, F., Zhao, C., Zhang, S., and Yang, M., "Thermal properties of poly(vinyl chloride)/montmorillonite nanocomposites", Polymer Degradation and Stability 84: (2004) 289-294 (2004). DOI: https://doi.org/10.1016/j.polymdegradstab.2003.11.003

[24] Zhu, R., Zhu, J., Ge, F., and Yuan, P., "Regeneration of spent organoclays after the sorption of organic pollutants: A review", Journal of Environmental Management, 90: 3212–3216, (2009). DOI: https://doi.org/10.1016/j.jenvman.2009.06.015

[25] Li, M., Wu, Z., and Ge, F., "A review of intercalation composite phase change material: Preparation, structure and properties", Renewable and Sustainable Energy Reviews, 16: 2094-2101, (2012). DOI: https://doi.org/10.1016/j.rser.2012.01.016

[26] Tournassat, C., Bizi, M., Braibant, G., and Crouzet, C., "Influence of montmorillonite tactoid size on Na-Ca cation exchange reactions", Journal of Colloid and Interface Science, 15: 443–454, (2011). DOI: https://doi.org/10.1016/j.jcis.2011.07.039

[27] Elashmawi, I.S., Elsayed, N.H., and Altalhi, F.A., "The changes of spectroscopic, thermal and electrical properties of PVDF/PEO containing lithium nanoparticles", Journal of Alloys and Compounds, 617: 877–883, (2014). DOI: https://doi.org/10.1016/j.jallcom.2014.08.088

[28] Chen, R.S., Ahmad, S., and Gan, S., "Characterization of recycled thermoplastics-based nanocomposites: Polymer-clay compatibility, blending procedure, processing condition, and clay content effects", Composites Part B: Engineering, 131: 87-97, (2017). DOI: https://doi.org/10.1016/j.compositesb.2017.07.057

[29] Fal, J., Bulanda, K., Oleksy, M., and Zyla, G., "Effect of bentonite on the electrical properties of a polylactide-based nanocomposite", Polymers, 16(10): 1372, (2024). DOI: https://doi.org/10.3390/polym16101372

[30] El-Khalafy, S.H., Hassanein, M.T., Alaskary, M.M., Ramzy, G.H., and Ali, A.I., "Synthesis, characterization, and dielectric properties of bentonite clay modified with (3-chloropropyl) triethoxysilane and Co(II) porphyrin complex for technological and electronic device applications", Materials Advances, 6: 1931–1949, (2025). DOI: https: //doi.org/ 10.1039/d4ma00982g